

# A receding contact problem of a layer resting on a half plane

Pembe Merve Karabulut<sup>\*</sup>, Gökhan Adıyaman<sup>a</sup> and Ahmet Birinci<sup>b</sup>

Department of Civil Engineering, Karadeniz Technical University, Trabzon, Turkey

(Received October 10, 2016, Revised July 13, 2017, Accepted August 18, 2017)

**Abstract.** In this paper, a receding contact problem for an elastic layer resting on a half plane is considered. The layer is pressed by two rectangular stamps placed symmetrically. It is assumed that the contact surfaces are frictionless and only compressive traction can be transmitted through the contact surfaces. In addition the effect of body forces is neglected. Firstly, the problem is solved analytically based on theory of elasticity. In this solution, the problem is reduced into a system of singular integral equations in which half contact length and contact pressures are unknowns using boundary conditions and integral transform techniques. This system is solved numerically using Gauss-Jacobi integral formulation. Secondly, two dimensional finite element analysis of the problem is carried out using ANSYS. The dimensionless quantities for the contact length and the contact pressures are calculated under various stamp size, stamp position and material properties using both solutions. The analytic results are verified by comparison with finite element results.

**Keywords:** receding contact; half plane; contact pressure; stamp; finite element method

## 1. Introduction

Contact problem is the one of the basic problems in the elasticity and has been widely studied due to its possible application to a variety of structures of practical interest such as foundation grillages, pavements in roads and runways, railway ballast, and other structures consisting of layered media. Numerous researchers have studied the contact problem using both numerical and analytical techniques. Most widely used numerical methods for contact mechanics are finite element method (Jing and Liao 1990, Satis Kumar *et al.* 1996) and boundary element method (Graciani *et al.* 2005, Paris *et al.* 1995). Additionally different analytical methods have been used to solve contact problems. Civelek and Erdogan (1976) considered frictionless contact problem for an elastic layer lying on a rigid foundation. Giannakopoulos and Pallot (2000) examined two dimensional contact of rigid cylinder on an elastic graded substrate. Guler and Erdogan (2007) investigated frictional sliding contact problems of rigid parabolic and cylindrical stamps on graded coatings. Chidlow and Teodorescu (2014) investigated sliding contact problems involving inhomogeneous materials comprising a coating-transition layer-substrate and rigid punch. Chen *et al.* (2015) studied frictional contact of a rigid punch on a half plane with shear modulus varying exponential gradient in an arbitrary direction. Turan *et al.* (2016) solved

axisymmetric contact problem of FG layer using analytical method, finite element method and stiffness matrix method. Two dimensional tractive rolling contact problem between a rigid cylinder and an orthotropic half plane is considered by Alina *et al.* (2017). Guler *et al.* (2017) solved the plane frictional contact problem of a cylindrical punch on a functionally graded orthotropic medium by using analytical and computational methods. Oner *et al.* (2017) examined continuous contact problem of a functionally graded layer resting on a elastic half plane.

Although in the majority of cases the contact area increases after the application of the load, there are others where the final contact area is smaller than the original, then such as contact is referred to as receding contact (Dundurs 1975). As a different point of view, a contact said to be a receding if the contact zone shrink as the two bodies are pressed against each other (Garrido and Lorenzana 1998). Several studies were performed on the receding contact problems. Keer *et al.* (1972) handled the smooth receding contact problem between an elastic layer and a half space under the assumption of the plane and axisymmetric cases. The frictionless contact problem for an elastic layer supported by two elastic quarter planes was studied Erdogan and Ratwani (1974). Gecit (1986) investigated axisymmetric contact problem of semi-infinite cylinder compressed against a half space. Salamon (1989) developed simple algorithm for simulation of structural elements in receding/advancing, unilateral contact with independent constraints. Gorrído *et al.* (1991) applied BEM to receding contact problem with friction. Gorrído and Lorenzana (1998) solved receding contact problem using boundary element method. Double receding contact problem between rigid stamp and two elastic layers was considered by Comez *et al.* (2004). El-Borgi *et al.* (2006) studied a frictionless receding contact plane problem between a functionally graded layer and a homogenous

<sup>\*</sup>Corresponding author, Ph.D. Student  
E-mail: [pembemerve.karabulut@ktu.edu.tr](mailto:pembemerve.karabulut@ktu.edu.tr)

<sup>a</sup>Ph.D. Student  
E-mail: [gadiyaman@ktu.edu.tr](mailto:gadiyaman@ktu.edu.tr)

<sup>b</sup>Professor  
E-mail: [birinci@ktu.edu.tr](mailto:birinci@ktu.edu.tr)

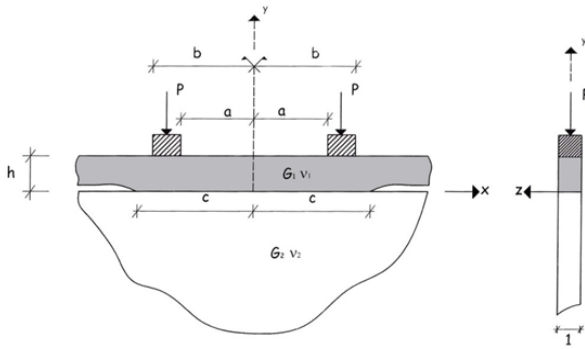


Fig. 1 Geometry and loading of the receding contact problem

half-space. The receding contact problem between an anisotropic elastic layer on anisotropic elastic half-plane was considered by Kahya *et al.* (2007). Rhimi *et al.* (2009) investigated the axisymmetric receding contact problem between a functionally graded layer and a homogeneous substrate. A double receding contact axisymmetric problem between a functionally graded layer and homogeneous half space is solved by Rhimi *et al.* (2011). Yaylacı and Birinci (2013) investigated receding contact problem for two elastic layers supported by two elastic quarter planes. El-Borgi *et al.* (2014) considered a frictional receding contact problem between a functionally graded layer and homogeneous half space. Receding contact problem for two elastic layers supported by a Winkler foundation was studied using analytical method and a finite element method by Oner *et al.* (2014). Comez (2015) is studied moving contact problem for a rigid cylindrical punch and a functionally graded layer. Yan and Li (2015) handled double receding contact plane problem between a functionally graded layer and an elastic layer. Adıyaman *et al.* (2015) is solved a receding contact problem analytically and numerically. Parel and Hills (2016) solved frictional receding contact problem of a layer on a half plane subjected to semi-infinite surface pressure and a receding contact problem for two layer functionally graded media is investigated by Comez *et al.* (2016).

In this paper, the frictionless and receding contact problem for an elastic layer resting on a half plane is solved using analytical method and a finite element method. Difference of this study than previous studies, first time, the effect of symmetric two stamps is examined in receding contact and the degree of accuracy is investigated by comparing numerical and analytical conclusions. The paper is organized as follows. In Section 2 and 3, the formulation and analytical solution of the problem is given, respectively.

A finite element model and finite element solution of the problem is described In Section 4, some of the calculated results obtained two different methods and compared with each other in Section 5. Finally, Section 6 summarizes the important conclusions of this study.

## 2. Formulation of the problem

As shown in Fig. 1, consider the symmetric plane strain

problem consists of an infinitely long homogeneous layer of thickness  $h$  resting on a half plane.  $G_1$  and  $\nu_1$  are the shear modulus and Poisson's ratio of the layer, respectively. Similarly,  $G_2$  and  $\nu_2$  are the shear modulus and Poisson's ratio of the half space, respectively.

The top of the layer is subjected to two concentrated load  $P$  by means of a rigid rectangular stamps replaced symmetrically. The main unknowns of the problem are the contact pressures, denoted  $p_1(x)$  and  $p_2(x)$ , over the contacts area between the stamp and the layer ( $a \leq x \leq b$ ) and between the layer and the half plane ( $0 \leq x \leq c$ ), respectively, and the receding contact half-length, namely  $c$ .

It is assumed that the contact surfaces are frictionless and only compressive traction can be transmitted through the contact surfaces. In addition,  $x=0$  is to be the plane of symmetry with respect to external loads as well as geometry, for simplicity. Clearly, it is sufficient to consider one half (i.e.,  $x \geq 0$ ) of the medium only.

For a plain strain problem, equilibrium equations with body forces neglected, the strain-displacement relationships and the linear elastic stress-strain law, respectively, given by

$$\frac{\partial \sigma_x}{\partial x} + \frac{\tau_{xy}}{\partial y} = 0, \quad \frac{\partial \tau_{yx}}{\partial x} + \frac{\partial \sigma_y}{\partial y} = 0, \quad (1a,b)$$

$$\varepsilon_{xx} = \frac{\partial u}{\partial x}, \quad \varepsilon_{yy} = \frac{\partial v}{\partial y}, \quad \varepsilon_{xy} = \frac{1}{2} \left( \frac{\partial u}{\partial y} + \frac{\partial v}{\partial x} \right), \quad (2a,b,c)$$

$$\sigma_x = \frac{G}{\kappa - 1} \left[ (1 + \kappa) \varepsilon_{xx} + (3 - \kappa) \varepsilon_{yy} \right], \quad (3a)$$

$$\sigma_y = \frac{G}{\kappa - 1} \left[ (3 - \kappa) \varepsilon_{xx} + (1 + \kappa) \varepsilon_{yy} \right], \quad (3b)$$

$$\tau_{xy} = 2G \varepsilon_{xy} \quad (3c)$$

where  $u$  and  $v$  are the  $x$  and  $y$  components of the displacement field, respectively;  $\sigma_x$ ,  $\sigma_y$  and  $\tau_{xy}$  are the components of the stress field in the same coordinate system;  $\varepsilon_{xx}$ ,  $\varepsilon_{yy}$  and  $\varepsilon_{xy}$  are the corresponding components of the strain field; and  $\kappa$  is a material property defined as  $\kappa = 3 - 4\nu$  for plane strain problems.

Combining Eqs. (1)-(3), the following two-dimensional Navier's equations are obtained

$$(\kappa + 1) \frac{\partial^2 u}{\partial x^2} + (\kappa - 1) \frac{\partial^2 u}{\partial y^2} + 2 \frac{\partial^2 v}{\partial x \partial y} = 0, \quad (4a)$$

$$(\kappa - 1) \frac{\partial^2 v}{\partial x^2} + (\kappa + 1) \frac{\partial^2 v}{\partial y^2} + 2 \frac{\partial^2 u}{\partial x \partial y} = 0. \quad (4b)$$

The boundary conditions for the problem can be defined as follows

$$\sigma_{y_1}(x, h) = -p_1(x)H(x-a)H(b-x), \quad 0 \leq x < \infty, \quad (5a)$$

$$\tau_{xy_1}(x, h) = 0, \quad 0 \leq x < \infty, \quad (5b)$$

$$\sigma_{y_1}(x, 0) = -p_2(x)H(c-|x|), \quad 0 \leq x < \infty, \quad (5c)$$

$$\tau_{xy_1}(x, 0) = 0, \quad 0 \leq x < \infty, \quad (5d)$$

$$\sigma_{y_2}(x, 0) = \sigma_{y_1}(x, 0), \quad 0 \leq x < \infty, \quad (5e)$$

$$\tau_{xy_2}(x, 0) = 0, \quad 0 \leq x < \infty, \quad (5f)$$

where  $H$  is the Heaviside function and sub-indices 1 and 2 represent the terms related to layer and half space, respectively. In addition, it is assumed that the stress field goes to zero at infinity

$$\sigma_y(x, y) = 0, \quad \tau_{xy}(x, y) = 0, \quad x^2 + y^2 \rightarrow \infty, \quad (6a,b)$$

Global equilibrium conditions for the problem can be expressed as

$$\int_a^b p_1(x_1) dx_1 = P, \quad \int_0^c p_2(x_2) dx_2 = P \quad (7a,b)$$

where  $P$  is concentrated load. In order to ensure continuity of the vertical displacement and eliminate rigid-body motion through the contact surfaces, the displacement field is subjected to following boundary conditions

$$\frac{\partial}{\partial x} [v_1(x, 0) - v_2(x, 0)] = 0, \quad 0 \leq x < c \quad (8a)$$

$$\frac{\partial}{\partial x} [v_1(x, h)] = 0, \quad a < x < b \quad (8b)$$

where  $v_1$  is the vertical displacement of the layer whereas  $v_2$  is the vertical displacement of the half plane.

### 3. Solution of the contact problem

Using symmetry considerations and Fourier transforms, the displacement components may be written

$$u(x, y) = F_s [\phi(\xi, y); \xi \rightarrow x] = \frac{2}{\pi} \int_0^\infty \phi(\xi, y) \sin(\xi x) dx \quad (9a)$$

$$v(x, y) = F_s [\psi(\xi, y); \xi \rightarrow x] = \frac{2}{\pi} \int_0^\infty \psi(\xi, y) \cos(\xi x) dx \quad (9b)$$

where  $\phi(\xi, y)$  and  $\psi(\xi, y)$  are the Fourier sine and Fourier cosine transforms of  $u$  and  $v$  with respect to the  $x$ -coordinate and  $y$ -coordinate, respectively. Substituting Eq. (9) into plane elasticity Eqs. (1)-(3), the following ordinary differential equations are obtained.

$$-(\lambda + 2G)\xi^2 \phi + G \frac{\partial^2 \phi}{\partial y^2} - (\lambda + G)\xi \frac{\partial \psi}{\partial y} = 0 \quad (10a)$$

$$(\lambda + 2G) \frac{\partial^2 \psi}{\partial y^2} - \xi^2 G \psi - (\lambda + G)\xi \frac{\partial \phi}{\partial y} = 0 \quad (10b)$$

The unknown functions  $\phi(\xi, y)$  and  $\psi(\xi, y)$  can be determined from the solution of the differential Eq. (10) as follows.

$$\phi(\xi, y) = (A_1 + A_2 y) e^{-\xi y} + (A_3 + A_4 y) e^{\xi y} \quad (11a)$$

$$\psi(\xi, y) = \left[ A_1 + \left( \frac{\kappa}{\xi} + y \right) A_2 \right] e^{-\xi y} +$$

$$\left[ -A_3 + \left( \frac{\kappa}{\xi} - y \right) A_4 \right] e^{\xi y} \quad (11b)$$

Substituting Eq. (11) into Eqs. (2),(3),(9), the displacement and stress field for homogeneous layer are obtained

$$u_1(x, y) = \frac{2}{\pi} \int_0^\infty \left[ (A_1 + A_2 y) e^{-\xi y} + (A_3 + A_4 y) e^{\xi y} \right] \sin(\xi x) d\xi \quad (12a)$$

$$v_1(x, y) = \frac{2}{\pi} \int_0^\infty \left\{ \left[ A_1 + \left( \frac{\kappa_1}{\xi} + y \right) A_2 \right] e^{-\xi y} + \left[ -A_3 + \left( \frac{\kappa_1}{\xi} - y \right) A_4 \right] e^{\xi y} \right\} \cos(\xi x) d\xi \quad (12b)$$

$$\frac{1}{2G_1} \sigma_{x_1}(x, y) = \frac{2}{\pi} \int_0^\infty \left\{ \left[ \xi (A_1 + A_2 y) - \left( \frac{3 - \kappa_1}{2} \right) A_2 \right] e^{-\xi y} + \left[ \xi (A_3 + A_4 y) + \left( \frac{3 - \kappa_1}{2} \right) A_4 \right] e^{\xi y} \right\} \cos(\xi x) d\xi \quad (13a)$$

$$\frac{1}{2G_1} \sigma_{y_1}(x, y) = \frac{2}{\pi} \int_0^\infty \left\{ - \left[ \xi (A_1 + A_2 y) + \left( \frac{1 + \kappa_1}{2} \right) A_2 \right] e^{-\xi y} + \left[ -\xi (A_3 + A_4 y) + \left( \frac{1 + \kappa_1}{2} \right) A_4 \right] e^{\xi y} \right\} \cos(\xi x) d\xi \quad (13b)$$

$$\frac{1}{2G_1} \tau_{xy_1}(x, y) = \frac{2}{\pi} \int_0^\infty \left\{ - \left[ \xi (A_1 + A_2 y) + \left( \frac{\kappa_1 - 1}{2} \right) A_2 \right] e^{-\xi y} + \left[ \xi (A_3 + A_4 y) - \left( \frac{\kappa_1 - 1}{2} \right) A_4 \right] e^{\xi y} \right\} \sin(\xi x) d\xi \quad (13b)$$

Similarly, for half plane, the stress field for homogeneous layer can be expressed as follows assuming the stress field goes to zero at infinity.

$$u_2(x, y) = \frac{2}{\pi} \int_0^\infty [B_1 + B_2 y] e^{\xi y} \sin(\xi x) d\xi \quad (14a)$$

$$v_2(x, y) = \frac{2}{\pi} \int_0^\infty \left[ -B_1 + \left( \frac{\kappa_2}{2} - y \right) B_2 \right] e^{\xi y} \cos(\xi x) d\xi \quad (14b)$$

$$\frac{1}{2G_2} \sigma_{x_2}(x, y) = \frac{2}{\pi} \int_0^\infty \left[ \xi (B_1 + B_2 y) + \left( \frac{3 - \kappa_2}{2} \right) B_2 \right] e^{\xi y} \cos(\xi x) d\xi \quad (15a)$$

$$\frac{1}{2G_2} \sigma_{y_2}(x, y) = \frac{2}{\pi} \int_0^\infty \left[ -\xi (B_1 + B_2 y) + \left( \frac{1 + \kappa_2}{2} \right) B_2 \right] e^{\xi y} \cos(\xi x) d\xi \quad (15b)$$

$$\frac{1}{2G_2} \tau_{xy_2}(x, y) = \frac{2}{\pi} \int_0^\infty \left[ \xi (B_1 + B_2 y) - \right]$$

$$\left(\frac{\kappa_2-1}{2}\right)B_2\Big]\sin(\xi x)d\xi \tag{15c}$$

Applying boundary conditions (5) to stress fields (13,15) the unknowns  $A_i$  ( $i=1,2,3,4$ ) and  $A_B$  ( $j=1,2$ ) can be found (given Appendix A). In addition, applying remaining displacement boundary conditions (8) yields to following singular integral equations, in which the unknowns are contact pressure between the layer and the rigid stamp  $p_1(t_1)$ , contact pressure between the layer and the half plane  $p_2(t_2)$ , and receding contact half-length  $c$

$$\int_a^b p_1(t_1)\left\{k_1(x_1,t_1)+\left[\frac{1}{t_1-x_1}+\frac{1}{t_1+x_1}\right]\right\}dt_1 + \int_{-c}^c p_2(t_2)k_2(x_1,t_2)dt_2 = 0 \tag{16a}$$

$$\int_a^b p_1(t_1)k_3(x_2,t_1)dt_1 + \int_{-c}^c p_2(t_2)\left\{k_4(x_2,t_2)+\left[\frac{1}{t_2-x_2}+\frac{1}{t_2+x_2}\right]\right\}dt_2 = 0 \tag{16b}$$

in which  $k_1, k_2, k_3$  and  $k_4$  are given in Appendix B.

#### 4. Numerical solution of singular integral equation

Using following dimensionless quantities, the numerical solution of the problem can be simplified.

$$z = \xi h \tag{17a}$$

$$x_1 = \frac{b-a}{2}s_1 + \frac{b+a}{2}, \quad t_1 = \frac{b-a}{2}s_1 + \frac{b+a}{2}, \tag{17b,c}$$

$$x_2 = \frac{c}{2}s_2, \quad t_2 = \frac{c}{2}r_2, \tag{17d,e}$$

$$\phi_1(r_1) = \frac{h}{P}p_1(t_1), \quad \phi_2(r_2) = \frac{h}{P}p_2(t_2) \tag{17f,g}$$

The singular Eq. (16) and equilibrium conditions (7) become

$$\frac{b-a}{2h} \int_{-1}^1 \phi_1(r_1) \left[ k_1(s_1, r_1) + \frac{1}{r_1 + s_1 + 2\frac{b+a}{b-a}} - \frac{1}{r_1 - s_1} \right] dr_1 + \frac{c}{h} \int_{-1}^1 \phi_2(r_2)k_2(s_1, r_1)dr_2 = 0 \tag{18a}$$

$$\int_{-1}^1 \phi_1(r_1) \left[ \frac{b-a}{2h}k_3(s_2, r_1) \right] dr_1 + \frac{c}{h} \int_{-1}^1 \phi_2(r_2)k_4(s_2, r_2)dr_2 = 0 \tag{18b}$$

$$\frac{b-a}{2h} \int_{-1}^1 \phi_1(r_1)dr_1 = 1, \quad \frac{c}{h} \int_{-1}^1 \phi_2(r_2)dr_2 = 2 \tag{19a,b}$$

It is clear to notice that contact surface between the layer and the rigid stamp has stress singularity at the both edges of the stamp ( $a,b$ ) (i.e.,  $\phi_1(-1)\rightarrow\infty, \phi_1(1)\rightarrow\infty$ ). As a result, the integral equation has a generalized Cauchy kernel with an index +1. For contact surface between the layer and the half plane, the integral equation has a generalized Cauchy kernel with an index -1 because of smooth contact at both ends ( $-c,c$ ) Hence, the solution may be sought described in Erdogan *et al.* (1973)

$$\phi_1(r) = w_1(r_i)g(r_i), \quad w_1(r_i) = (1-r_i^2)^{-0.5}, \quad -1 \leq r_i \leq 1, \quad (i = 1, \dots, N), \tag{20a,b}$$

$$\phi_2(r) = w_2(r_{2i})g(r_{2i}), \quad w_2(r_{2i}) = (1-r_{2i}^2)^{0.5}, \quad -1 \leq r_{2i} \leq 1, \quad (i = 1, \dots, N) \tag{21a,b}$$

Using appropriate Gauss–Jacobi integration formulas, the solution of Eqs. (18),(19) may be expressed as a system of algebraic equations

$$\sum_{i=1}^N W_{1i}g_1(r_{1i}) \left[ \frac{b-a}{2h}k_1(s_{1k}, r_{1i}) + \frac{1}{r_{1i} + s_{1k} + 2\frac{b-a}{b+a}} - \frac{1}{r_{1i} - s_{1k}} \right] + \sum_{i=1}^N W_{2i}^N g_{2i}(r_{2i}) \frac{c}{h}k_2(s_{2k}, r_{2i}) = 0 \quad (k=1, \dots, N-1) \tag{22a}$$

$$\sum_{i=1}^N W_{1i}g_1(r_{1i}) \frac{b-a}{2h}k_3(s_{2k}, r_{1i}) + \sum_{i=1}^N W_{2i}g_2(r_{2i}) \left[ \frac{c}{h}k_4(s_{2k}, r_{2i}) + \frac{1}{r_{2i} - s_{2k}} \right] = 0 \quad (k=1, \dots, N) \tag{22b}$$

$$\frac{b-a}{2h} \sum_{i=1}^N W_{1i}g_1(r_{1i}) = 1 \tag{23a}$$

$$\frac{c}{h} \sum_{i=1}^N W_{2i}g_1(r_{2i}) = 2 \tag{23b}$$

where  $r_{1i}, r_{2i}, s_{1k}, s_{2k}, W_{1i}$ , and  $W_{2i}$  are known constants as shown in Appendix C.

Note that the system of algebraic Eq. (22) are consist of  $(2N-1)$  equations in total for  $(2N+1)$  unknowns namely  $g_{1i}, g_{2i}$  ( $i=1, \dots, N$ ) and  $c$ . In order to solve for  $(2N+1)$  unknowns, in addition to the system of equations given by (22), the global equilibrium conditions (23) are also used. Thus, the solution of the problem is reduced into the solution of the system consists of  $(2N+1)$  equations for  $(2N+1)$  unknowns. Note that the system is highly nonlinear in  $c$ , and an iterative procedure have to be used in order to determine these unknowns. In this procedure, firstly a prediction for unknown  $c$  is made and then a new value is chosen repeatedly until the value  $c$  satisfies the equilibrium conditions.

#### 5. Finite element solution

In section 4, contact pressures are obtained by means of analytical method. Contact mechanics analyses are also

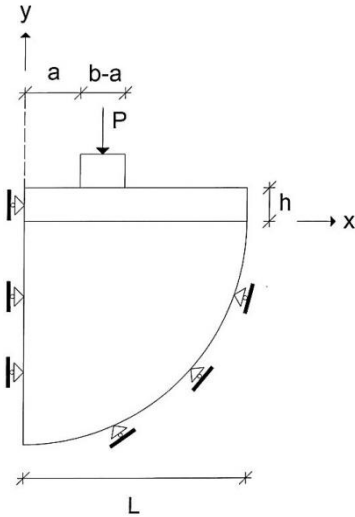


Fig. 2 The geometry for the analysis

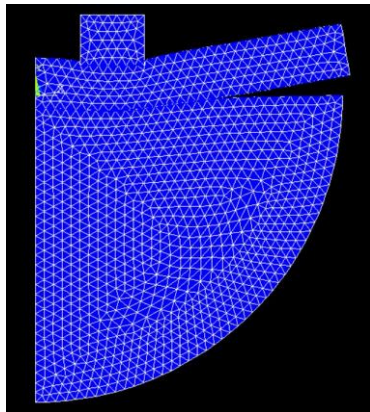


Fig. 3 Deformed geometry for FEM analysis

performed using finite element method. In the FEM, structures are divided into a large number of predetermined elements and a lot of equation sets are attained combining this elements. With recent developments in computer technology and commercial package programs for FEM, solution of large number of equation sets is accomplished.

In the literature, plane strain problems were modeled two dimensional (2D) instead of three dimensional (3D) due to very close results are obtained in both cases. (Ethison *et al.* 2005, Brizmer *et al.* 2006) Therefore two dimensional finite element model has been used in this study. Due to the problem exhibits symmetry in geometry, material proportions and loading, only half of the problem is modeled. Because of the horizontal displacement is zero on the symmetry axis, horizontal component of displacement ( $U_x$ ) is restricted throughout this surface. In addition, since displacement components becomes zero at infinity for the half plane,  $U_x$  and  $U_y$  (displacements in  $x$  and  $y$  directions) is restricted throughout the bottom surface of the half plane in the finite element model. The geometry and the applied load are shown symmetrically in Fig. 2 and the finite element model before analysis in Fig. 3. In the analyses, geometric properties are taken as  $L=10$  m (length of the layer in  $x$  direction),  $h=1$  m (thickness of the layer in  $x$  direction) and material properties are taken as  $E_1=10000$

Table 1 The variation of  $c/h$  for various  $G_1/G_2$  and  $(b+a)/2h$

$G_1/G_2$	$c/h$									
	$(b+a)/(2h) = -0.75$		$(b+a)/(2h) = 1$		$(b+a)/(2h) = 1.25$		$(b+a)/(2h) = 1.5$		$(b+a)/(2h) = 1.75$	
	Ana.	FEM	Ana.	FEM	Ana.	FEM	Ana.	FEM	Ana.	FEM
0.05	1.9197	1.9853	2.1816	2.0761	2.4393	2.1816	2.6924	2.2968	2.9432	2.4179
0.1	1.9436	2.0087	2.2057	2.1000	2.4620	2.2060	2.7175	2.3205	2.9687	2.4425
0.2	1.9890	2.0531	2.2517	2.1538	2.5110	2.2501	2.7655	2.3679	3.0173	2.4895
0.4	2.0731	2.1370	2.3361	2.2287	2.5972	2.2292	2.8540	2.4529	3.1067	2.5753
1	2.2818	2.3398	2.5458	2.4356	2.8099	2.5925	3.0703	2.6648	3.3269	2.7887
2	2.5419	2.5861	2.8061	2.6906	3.0717	2.8548	3.3350	2.9281	3.5948	3.0542
4	2.9036	2.9267	3.1676	3.0440	3.4333	3.1675	3.6980	3.2939	3.9603	3.4219

\*( $b+a)/(2h)=0.75, \kappa_1=\kappa_2=2$ .

MPa,  $\nu_1=0.25$ . Other parameters are chosen compatible with analytical values. PLANE 183 elements are used for the modeling elastic layer and half plane. PLANE 183 element consist of eight nodes and per nodes have two degree of freedoms: translations in the nodal  $x$  and  $y$  directions.

Augmented Lagrangian Method is used as the contact algorithm and contact areas are meshed by surface the surface contact elements: CONTA 172 and TARGE 169. CONTA 172 is used to represent the mechanical contact analysis. The target surface, defined by TARGE 169, was, therefore, used to represent 2D target surfaces for the associated contact elements CONTA 172 (Sofuoglu and Ozer 2008). A mesh refinement study is performed to decrease the percent error of solutions and determine the optimum mesh size for FEM. The percent error of solutions is checked for all models untill stable values and minimum errors are achieved, corresponding model obtained by mesh refinement study is used for all remaining finite element analysis.

## 6. Numerical results

The geometry and loading of the problem are given in Fig. 1. The height of the layer  $h$  is taken as 1. In addition, iterations are continued until the accuracy is less than  $10^{-5}$  for  $N=20$ . Some calculated results for contact distance and contact pressures obtained using analytical and finite element solution are shown in Tables 1, 2 and Figs. 4-10. Note that all quantities are dimensionless.

Table 1 shows the half contact lengths  $c/h$  for various shear moduli ratios  $G_1/G_2$  and the distance of the stamp from the symmetry axis  $(b+a)/2h$ . It is seen from the table that for a fixed value of  $G_1/G_2$ ,  $c/h$  increases for increasing  $(b+a)/2h$ . Similarly for a fixed  $(b+a)/2h$ , increasing  $G_1/G_2$  results in an increment of the contact length.

The variation of the half contact length  $c/h$  for various shear moduli ratios  $G_1/G_2$  and the width of the stamp  $(b-a)/h$  is given in Table 2. It can be concluded that for a fixed values of  $G_1/G_2$ ,  $c/h$  increases for increasing  $(b-a)/h$ .

Figs. 4 and 5 show the variation of the contact pressure distribution between the layer and the stamp contact surface ( $p_1(x_1)/(P/h)$ ) and the variation of the contact pressure

Table 2 The variation of  $c/h$  for various  $G_1/G_2$  and  $(b-a)/h$

$G_1/G_2$	$c/h$									
	$(b-a)/h=0.25$		$(b-a)/h=0.5$		$(b-a)/h=0.75$		$(b-a)/h=1$		$(b-a)/h=1.5$	
	Ana.	FEM	Ana.	FEM	Ana.	FEM	Ana.	FEM	Ana.	FEM
0.05	1.8700	1.9000	1.9149	1.9500	1.9853	2.0125	2.0761	2.1000	2.2968	2.3125
0.1	1.8936	1.9250	1.9384	1.9625	2.0087	2.0375	2.1000	2.1125	2.3205	2.3375
0.2	1.9385	1.9625	1.9837	2.0125	2.0531	2.0750	2.0538	2.1625	2.3679	2.3750
0.4	2.0205	2.0375	2.0663	2.0750	2.1370	2.1500	2.2287	2.2375	2.4529	2.4500
1	2.2159	2.2125	2.2642	2.2500	2.3398	2.3250	2.4356	2.4125	2.6648	2.6250
2	2.4420	2.4250	2.5005	2.4625	2.5861	2.5500	2.6906	2.6375	2.9281	2.8625
4	2.7442	2.6875	2.8218	2.7500	2.9267	2.8500	3.0440	2.9500	3.2939	3.1875

\*( $b+a$ )/( $2h$ )=1.25,  $\kappa_1=\kappa_2=2$ .

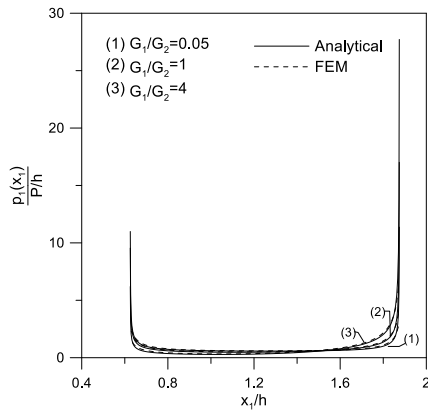


Fig. 4 The variation of the  $p_1(x_1)/(P/h)$  for various  $G_1/G_2$  ( $(b-a)/h=1.25$ ,  $(b+a)/(2h)=1.25$ ,  $\kappa_1=\kappa_2=2$ )

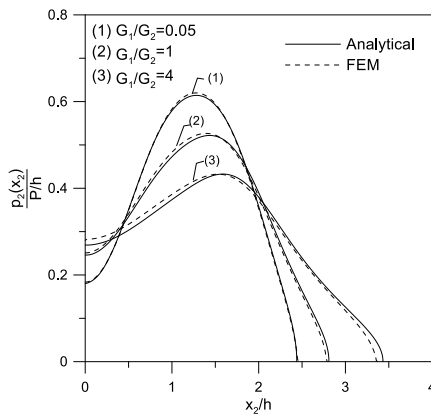


Fig. 5 The variation of the  $p_2(x_2)/(P/h)$  for various  $G_1/G_2$  ( $(b-a)/h=1.25$ ,  $(b+a)/(2h)=1.25$ ,  $\kappa_1=\kappa_2=2$ )

distribution between the layer and the half plane contact surface ( $p_2(x_2)/(P/h)$ ) for various shear moduli ratios  $G_1/G_2$ , respectively. It may be observed that  $p_1(x_1)/(P/h)$  goes to infinite at the end of the contact zone in Fig. 4. Significant changes aren't observed on the contact stress distributions between the elastic layer and rigid stamps for increasing values of  $G_1/G_2$ . It can be seen from Fig. 5 that the peak value of the stress decreases for increasing values of  $G_1/G_2$ , whereas the stress values on the symmetry axis increase. In addition, the position of the peak value move away from the symmetry axis for increasing  $G_1/G_2$ .

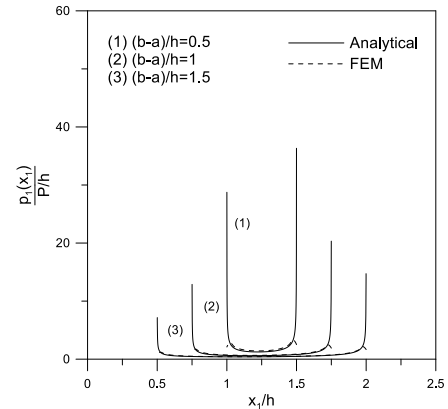


Fig. 6 The variation of the  $p_1(x_1)/(P/h)$  for various  $(b-a)/h$  ( $(b+a)/(2h)=1.25$ ,  $G_1/G_2=4$ ,  $\kappa_1=\kappa_2=2$ )

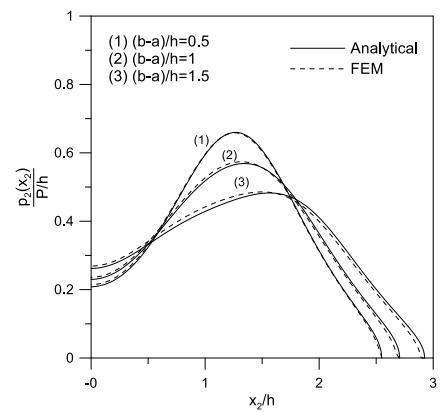


Fig. 7 The variation of the  $p_2(x_2)/(P/h)$  for various  $(b-a)/h$  ( $(b+a)/(2h)=1.25$ ,  $G_1/G_2=4$ ,  $\kappa_1=\kappa_2=2$ )

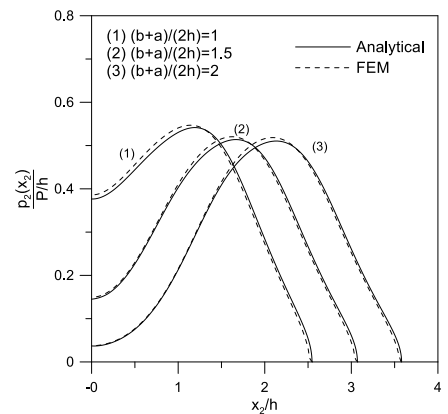


Fig. 8 The variation of the  $p_2(x_2)/(P/h)$  for various  $(b+a)/(2h)$  ( $(b-a)/h=1.25$ ,  $G_1/G_2=4$ ,  $\kappa_1=\kappa_2=2$ )

The variation of the  $p_1(x_1)/(P/h)$  and  $p_2(x_2)/(P/h)$  for various  $(b-a)/h$ , are given in Figs. 6 and 7, respectively. From Fig. 6,  $p_1(x_1)/(P/h)$  decreases near the edge of the stamp for increasing  $(b-a)/h$  values. It can be concluded from Fig. 7 that increasing stamp width results in a reduction of the maximum stresses whereas the stresses on the symmetry axis increase. In addition, the distance between the symmetry axis and the position of the peak value increases.

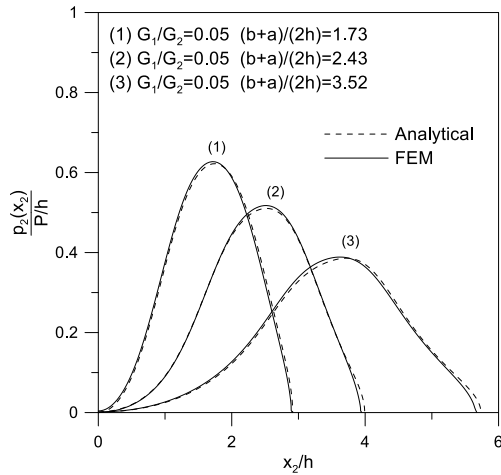


Fig. 9 The variation of the  $p_2(x_2)/(P/h)$  for various  $G_1/G_2$  and  $(b+a)/(2h)$  ( $(b-a)/h=1.25$ ,  $\kappa_1=\kappa_2=2$ )

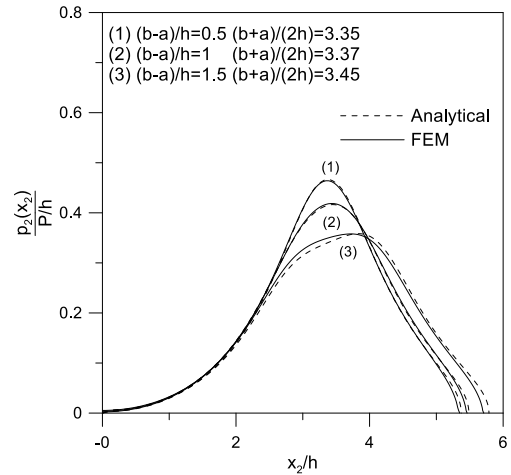


Fig. 10 The variation of the  $p_2(x_2)/(P/h)$  for various  $(b-a)/h$  and  $(b+a)/(2h)$  ( $G_1/G_2=4$ ,  $\kappa_1=\kappa_2=2$ )

Fig. 8 shows the variation of the contact pressure distribution between the layer and the half plane contact surface ( $p_2(x_2)/(P/h)$ ) for various distances of the stamp from the symmetry axis  $(b+a)/2h$ . It can be seen from Fig. 8, if distance of stamps from the origin increases, peak value of stresses move away from the symmetry axis and the stress values on the symmetry axis decreases.

The variation of  $p_2(x_2)/(P/h)$  providing that the stress value on the symmetry axis goes to zero, i.e., the separation starts at the symmetry axis between the layer and the half space, for various  $G_1/G_2$  and  $(b+a)/(2h)$  is given in Fig.9. The peak value of the stress decreases while the distance between the symmetry axis and the position of the peak value increases for increasing  $G_1/G_2$  and  $(b+a)/(2h)$  values.

Fig. 10 shows the variation of  $p_2(x_2)/(P/h)$  providing that the stress value on the symmetry axis goes to zero for various  $(b-a)/h$  and  $(b+a)/(2h)$ . It can be concluded that, the peak value of the stress decreases while the distance between symmetry axis and the position of the peak value increases for increasing punch length and  $(b+a)/(2h)$ .

It is seen from all tables and figures that dimensionless contact half lengths and contact pressures distributions obtained from analytical solution and finite element solution agree very well.

## 7. Conclusions

In this paper, a frictionless receding contact of an elastic layer resting on homogenous half plane was considered. The layer was subjected to concentrated loads by means of rectangular stamps placed symmetrically. For analytical solution, using Fourier cosine and Fourier sine transforms the problem was converted into the solution of a Cauchy-type singular integral equations in which the contact pressures and the receding contact half-length were the unknowns. The singular integral equation was solved numerically using Gauss-Jacobi integration formulation. An iterative procedure was employed to obtain the correct receding contact half-length that satisfies the global equilibrium condition. Two dimensional finite element

analysis of the problem is carried out using ANSYS. The effect of stamp size, stamp position and material properties on the contact pressure and on the half contact length were investigated using a parametric study. It is also verified that the difference between analytical solution and finite element solution carried out by ANSYS is in an acceptable range.

## References

- Adiyaman, A., Yaylaci, M. and Birinci, A. (2015), "Analytical and finite element solution of a receding contact problem", *Struct.Eng. Mech.*, **54**(1), 69-85.
- Alina, Y., Zakerhaghighi, H., Abdinzaziri, S. and Guler, M.A. (2017), "Rolling contact problem for an orthotropic medium", *Acta Mechanica*, **228**, 447-464.
- Brizmer, V., Kligerman, Y. and Etsion, I. (2006), "The effect of contact conditions and material properties on the elasticity terminus of a spherical contact", *Int. J. Solid. Struct.*, **43**, 5736-5749.
- Chen, P., Chen, S. and Peng, J. (2015), "Frictional contact of a rigid punch on an arbitrarily oriented gradient half plane", *Acta Mechanica*, **226**, 4207-4221.
- Chidlow, S.J. and Teodorescu, M. (2014), "Sliding contact problems involving inhomogeneous materials comprising a coating-transition layer-substrate and a rigid punch", *Int. J. Solid. Struct.*, **51**, 1931-1949.
- Civelek, M.B. and Erdogan, F. (1976), "Interface separation in a frictionless contact problem for an elastic layer", *J. Appl. Mech.*, **43**(1), 175-177.
- Comez, I. (2015), "Contact problem for functionally graded layer intended by a moving punch", *Int. J. Mech. Sci.*, **100**, 339-344.
- Comez, I., El-Borgi, S., Kahya, V. and Erdol, R. (2016), "Receding contact problem for two-layer functionally graded media intended by a rigid punch", *Acta Mechanica*, **227**(9), 2493-2504.
- Dundurs, J. (1975), *Properties of Elastic Bodies In Contact*, Delft University Press, Delft, Netherlands.
- El-Borgi, S., Abdelmaula, R. and Keer, L. (2006), "A receding contact plane problem between a functionally graded layer and a homogeneous substrate", *Int. J. Solid. Struct.*, **43**(3-4), 658-674.
- El-Borgi, S., Usman, S. and Guler, M.A. (2014), "A frictional receding contact plane problem between functionally graded

- layer and a homogeneous substrate”, *Int. J. Solid. Struct.*, **51**(25-26), 4462-4476.
- Erdogan, F. and Gupta, G. (1972), “On the numerical solution of singular integral equations”, *Quart. Appl. Math.*, **29**, 525-534.
- Erdogan, F. and Ratwani, M. (1974), “Contact problem for an elastic layer layer supported by two elastic quarter planes”, *J. Appl. Mech. Tran. ASME*, **41**(3), 673-678.
- Etsion, I., Kligerman, Y. and Kadin, Y. (2005), “Unloading of an elastic-plastic loaded spherical contact”, *Int. J. Solid. Struct.*, **42**, 3716-3729.
- Gecit, M.R. (1986), “The axisymmetrical double contact problem for and frictionless elastic layer intended by an elastic cylinder”, *Int. J. Eng. Sci.*, **24**(9), 1571-1584.
- Giannakopoulos, A.E. and Pallot, P. (2000), “Two-dimensional contact analysis of elastic graded materials”, *J. Mech. Phys. Solid.*, **48**, 1597-1631.
- Gorrdo, J.A. and Foces, A. (1991), “BEM applied to receding contact problems with frictions”, *M.d Comput. Model.*, **15**(3-5), 143-153.
- Gorrdo, J.A. and Lorenzana, A. (1998), “Receding contact problem involving large displacement using the BEM”, *Eng. Anal. Bound. Elem.*, **21**(4), 295-303.
- Graciani, E., Mantic, C., Paris, F. and Blazquez, A. (2005), “Weak formulation of axisymmetric frictionless contact problems with boundary elements: Application to interface cracks”, *Comput. Struct.*, **83**(10-11), 836-855.
- Guler, M.A. and Erdogan, F. (2007), “The frictional sliding contact problems of rigid parabolic and cylindrical stamps on graded coatings”, *Int. J. Mech. Sci.*, **49**(2), 161-182.
- Guler, M.A., Kucuksucu, A., Yilmaz, K.B. and Yildirim, B. (2017), “On the analytical and finite element solution of plane contact problem of a rigid cylindrical punch sliding over a functionally graded orthotropic medium”, *Int. J. Mech. Sci.*, **120**, 12-29.
- Jing, H.S. and Liao, M.L. (1990), “An improved finite element scheme for elastic contact problems with friction”, *Comput. Struct.*, **35**(5), 571-578.
- Kahya, V., Ozsahin, T., Birinci, A. and Erdol, R. (2007), “A receding contact for an anisotropic elastic medium consisting of a layer and a half plane”, *Int. J. Solid. Struct.*, **44**(17), 5695-5710.
- Keer, L.M., Dundurs, J. and Tsai, K.C. (1972), “Problems involving a receding contact between a layer and a half space”, *J. Appl. Mech.*, **39**(4), 1115-1120.
- Oner, E., Adiyaman, G. and Birinci, A. (2017), “Continuous contact problem of a functionally graded layer resting on an elastic half-plane”, *Arch. Mech.*, **69**, 53-73.
- Oner, E., Yaylaci, M. and Birinci, A. (2014), “Solution of receding contact problem using analytical method and a finite element method”, *J. Mech. Mater. Struct.*, **9**(3), 333-345.
- Parel, K.S. and Hills, D.A. (2016), “Frictional receding contact analysis of a layer on a half plane subjected to semi-infinite surface pressure”, *Int. J. Mech. Sci.*, **108-109**, 137-143.
- Paris, F., Blazquez, A. and Canas, J. (1995), “Contact problems with nonconforming discretizations using boundary element method”, *Comput. Struct.*, **57**(5), 829-839.
- Rhimi, M., El-Borgi, S. and Lajnef, N. (2011), “A double receding contact axisymmetric problem between a functionally graded layer and a homogeneous substrate”, *Mech. Mater.*, **43**(12), 787-798.
- Rhimi, M., El-Borgi, S., Ben Said, W. and Ben Jemaa, F. (2009), “A receding contact axisymmetric problem between a functionally graded layer and a homogeneous substrate”, *Int. J. Solid. Struct.*, **46**(20), 3633-3642.
- Salamon, N.J. (1989), “Receding advancing contact of structural elements simplified”, *Comput. Struct.*, **33**(2), 509-512.
- Satis Kumar, K., Dattaguru, B., Ramamurthy, T.S. and Raju, K.N. (1996), “Elasto-plastic contact stress analysis of joints subjected to cycling loading”, *Comput. Struct.*, **60**(6), 1067-1077.
- Sofoglu, H. and Ozer, A. (2008), “Thermomechanical analysis of elastoplastic medium in sliding contact with fractal surface”, *Tribology Int.*, **41**(8), 783-796.
- Turan, M., Adiyaman, G., Kahya, V. and Birinci, A. (2016), “Axisymmetric analysis of a functionally graded layer resting on elastic substrate”, *Struct. Eng. Mech.*, **58**(3), 423-442.
- Yan, J. and Li, X. (2015), “Double receding contact plane problem between a functionally graded layer and an elastic layer”, *Eur. J. Mech. A/Solid.*, **53**, 143-150.
- Yaylaci, M. and Birinci, A. (2014) “The receding contact problem of two elastic layers supported by two elastic quarter planes”, *Struct. Eng. Mech.*, **48**(2), 241-255.

CC

**Appendix A**

The unknowns  $A_i$  ( $i=1,2,3,4$ ) and  $B_j$  ( $j=1,2$ ) can be written as follows

$$A_1 = \frac{1}{2\Delta\xi} e^{\xi h} [P_1(\xi)A_{11} + P_2(\xi)A_{12}] \tag{A.1}$$

$$A_2 = \frac{1}{\Delta} e^{\xi h} [P_1(\xi)A_{21} + P_2(\xi)A_{22}] \tag{A.2}$$

$$A_3 = \frac{1}{2\Delta\xi} e^{\xi h} [P_1(\xi)A_{31} + P_2(\xi)A_{32}] \tag{A.3}$$

$$A_4 = \frac{1}{\Delta} e^{\xi h} [P_1(\xi)A_{41} + P_2(\xi)A_{42}] \tag{A.4}$$

$$B_1 = \frac{1}{2\xi} P_2(\xi)B_{11} \tag{A.5}$$

$$B_2 = P_2(\xi)B_{21} \tag{A.6}$$

where  $A_{11}, A_{12}, A_{21}, A_{22}, A_{31}, A_{32}, A_{41}, A_{42}, B_{11}, B_{12}$ , and  $\Delta$  are known functions.

$$A_{11} = -(\kappa_1 + e^{2\xi h} - \kappa_1 e^{2\xi h} + 2\xi h - 2h\kappa_1\xi e^{2\xi h} - 1) \tag{A.7}$$

$$A_{12} = -\frac{G_2}{G_1} e^{h\xi} (\kappa_1 e^{2\xi h} - e^{2\xi h} - \kappa_1 + 4h^2\xi^2 - 2h\xi + 2h\kappa_1\xi + 1) \tag{A.8}$$

$$A_{21} = \frac{G_2}{G_1} e^{h\xi} (e^{2h\xi} + 2h\xi - 1) \tag{A.9}$$

$$A_{22} = -(e^{2\xi h} + 2h\xi e^{2\xi h} - 1) \tag{A.10}$$

$$A_{31} = (\kappa_1 + e^{2\xi h} - \kappa_1 e^{2\xi h} - 2h\kappa_1\xi + 2h\xi e^{2\xi h} - 1) \tag{A.11}$$

$$A_{32} = -\frac{G_2}{G_1} e^{-h\xi} (\kappa_1 e^{2\xi h} + e^{2\xi h} - \kappa_1 e^{2\xi h} + 4h^2\xi^2 e^{2\xi h} + 2h\xi e^{2\xi h} - 2h\kappa_1\xi e^{2\xi h} + 1) \tag{A.12}$$

$$A_{41} = -(e^{2h\xi} + 2h\xi - 1) \tag{A.13}$$

$$A_{42} = \frac{G_2}{G_1} e^{-h\xi} (e^{2\xi h} + 2h\xi e^{2\xi h} - 1) \tag{A.14}$$

$$B_{11} = (\kappa_2 - 1) \tag{A.15}$$

$$B_{21} = 1 \tag{A.16}$$

$$\Delta = (2e^{4h\xi} - e^{4h\xi} + 4h^2\xi^2 e^{2h\xi} - 1) \tag{A.17}$$

**Appendix B**

$k_1, k_2, k_3$  and  $k_4$  are given as:

$$k_1(x_1, t_1) = \int_0^\infty \frac{1}{\Delta} (2 - 2e^{4h\xi} - 8h\xi e^{2h\xi} - 2)\sin(\xi x_1)\cos(\xi t_1)d\xi \tag{B.1}$$

$$k_2(x_1, t_2) = \int_0^\infty \frac{1}{\Delta} (-2e^{3h\xi} + 2e^{h\xi} - 2h\xi e^{h\xi} - 2h\xi e^{3h\xi})\sin(\xi(t_2 - x_1))d\xi \tag{B.2}$$

$$k_3(x_2, t_1) = \frac{1}{1+\beta} \int_0^\infty \frac{1}{\Delta} (4e^{h\xi} - 4e^{3h\xi} - 4h\xi e^{h\xi} - 4h\xi e^{3h\xi})\sin(\xi x_2)\cos(\xi t_1)d\xi \tag{B.3}$$

$$k_4(x_2, t_2) = \frac{1}{1+\beta} \int_0^\infty \frac{1}{\Delta} (-e^{4h\xi} - 4h\xi e^{2h\xi} + 1) - 1]\sin(\xi(t_2 - x_2))d\xi \tag{B.4}$$

**Appendix C**

$r_{1i}, r_{2i}, s_{1k}, s_{2k}, W_{1i}$ , and  $W_{2i}$  can be described as follows:

$$r_{1i} = \cos\left(\pi \frac{i-1}{N-1}\right), \quad r_{2i} = \cos\left(\pi \frac{i}{N+1}\right) \quad (i = 1, \dots, N), \tag{C.1a,b}$$

$$s_{1k} = \cos\left(\pi \frac{2k-1}{2N-2}\right), \quad s_{2k} = \cos\left(\pi \frac{2k-1}{2N+1}\right) \quad (k = 1, \dots, N-1) \tag{C.2a,b}$$

$$W_{1i} = \frac{\pi}{N-1} \quad (i = 2, \dots, N), \tag{C.3}$$

$$W_1 = W_N = \frac{\pi}{2(N-1)} \tag{C.4}$$

$$W_{2i}^N = \frac{1-r_{2i}^2}{N+1} \quad (i = 1, \dots, N) \tag{C.5}$$